



EXPERIMENTAL AND NUMERICAL INVESTIGATION ON THE EFFECT OF INFILL WALLS ON DYNAMIC BEHAVIOR IN RC STRUCTURES: SHAKE TABLE TESTS

^{1,*} Abdulhamit NAKİPOĞLU , ² M. Sami DÖNDÜREN 

Konya Technical University, Engineering and Natural Sciences Faculty, Civil Engineering Department, Konya, TÜRKİYE

¹anakupoglu@ktun.edu.tr, ²msdonduren@ktun.edu.tr

Highlights

- RC frame samples tested with and without infill walls.
- Shake table experiments were conducted, and numerical analysis was performed in ETABS program.
- Both experimental modal analyses and load-displacement analyses were carried out.
- Effects of infill walls on dynamic behavior were studied.
- Infill walls greatly increased stiffness and decreased displacements substantially.



EXPERIMENTAL AND NUMERICAL INVESTIGATION ON THE EFFECT OF INFILL WALLS ON DYNAMIC BEHAVIOR IN RC STRUCTURES: SHAKE TABLE TESTS

^{1,*} Abdulhamit NAKİPOĞLU , ² M. Sami DÖNDÜREN 

Konya Technical University, Engineering and Natural Sciences Faculty, Civil Engineering Department, Konya, TÜRKİYE

¹ anakipoglu@ktun.edu.tr, ² msdonduren@ktun.edu.tr

(Received: 11.12.2024; Accepted in Revised Form: 12.02.2025)

ABSTRACT: Infill walls have many positive and negative effects on reinforced concrete (RC) buildings under the effect of earthquakes, but these are often not taken into consideration sufficiently. The contribution of walls to stability and stiffness in particular is considerable. In the negative sense, due to various reasons, incorrect/incomplete use of infill walls can cause extremely fatal irregularities such as short columns and soft stories. In this study, the effect of infill walls on the dynamic behavior of reinforced concrete buildings was examined. The study was conducted on a dynamic basis in order to approach the behavior under the effect of earthquakes in a more realistic way. For this purpose, a 1/3 scale 2-storey single-span reinforced concrete frame was produced for the experiments. Forced vibration tests were carried out on the shake table in the reference state (bare frame) and in the infill-walled state. The sample was subjected to an artificial ground motion with a peak ground acceleration (PGA) value of 0.54 g in both states. Experimental modal analysis, load-displacement analysis, and numerical analysis on ETABS structural analysis software were done. As a result, it was observed that the infill walls significantly enhanced the stiffness, leading to a considerable reduction in displacement values. Calculations showed that the natural frequencies increased by approximately 5-10%, while the global damping ratio decreased by about 20%.

Keywords: *Dynamic Behavior, Dynamic Characteristics, ETABS, Experimental Modal Analysis, Infill Wall, Shake Table*

1. INTRODUCTION

Earthquake resistant structural design is a very sensitive issue for Turkey. To reduce the impact of earthquakes on structures, advancements made in engineering designs and structural material technology have led to the development of lighter and stronger materials. However, the use of such materials in structural systems reduces the cross-sections and makes the systems slender. In addition, the increases obtained in strength are not at the same rate in the elasticity modulus, which is one of the most important parameters of stiffness. This situation causes significant decreases in the stiffness of the elements and systems. Therefore, the decreased stiffness creates serious vibration and stability problems in the structures and increases the interaction of the structures with their surroundings, namely the soil, under the effect of time-dependent dynamic loads such as earthquakes.

The effect of infill walls in buildings is often not given enough importance. Although infill walls do not contribute much to the structure in terms of strength, which is at most 15% according to the Turkish Building Earthquake Code TBEC 2018 [1], they provide serious gains in terms of stability. Infill walls, which greatly increase the system stiffness, also significantly limit lateral drifts. The contribution of infill walls to the system is largely in undamaged/elastic state, and the stiffness of walls decreases significantly with cracking with brittle behavior, and therefore their contribution to the strength and the stiffness decreases significantly in the plastic region. A critical issue is the correct use of infill walls. Walls should be constructed as symmetrically as possible on each story of the building. Otherwise, for example, in a building constructed with no ground story walls for commercial purposes and all other floors with infill walls, soft story irregularity (stiffness irregularity between adjacent stories) is almost

*Corresponding Author: Abdulhamit NAKİPOĞLU, anakipoglu@ktun.edu.tr

inevitable. Another example is the formation of short columns as a result of the application of band-type windows or the partial application of infill walls on the story instead of the entire story height for some other reason. Both situations cause a large part of the earthquake energy to be concentrated in these areas and often cause the structure to collapse [1], [2], [3].

Dynamic loads on structures such as earthquakes are often analyzed with static solution methods. The reason for this is usually the complexity of the solution created by the inertial forces that arise as a result of dynamic effects. However, in order to see the real behavior of a system under dynamic loads, the solution method must also be dynamic-based [4].

Although many experimental studies have been conducted on the contribution of infill walls to the behavior of the system in buildings, the vast majority of these are static-based studies. In the studies mentioned here, mostly static, or quasi-static reversed-cyclic loading type were used. Zhang et al. [5] studied on failure mechanism and seismic performance of reinforced concrete (RC) frame infilled walls structures reinforced by carbon fiber reinforced plastics (CFRP), Ou et al. [6] investigated cyclic behavior and pushover analysis of large scale two-bay, two-story reinforced concrete frames infilled with walls with openings, Jin et al. [7] investigated in-plane and out-of-plane interaction of isolated infills in reinforced concrete frames, Pradhan et al. [8] studied effects of passive confinement on out-of-plane robustness of unreinforced masonry infill walls, Monical and Pujol [9] studied the response of reinforced concrete frames with and without masonry infill walls to earthquake motions, Bhaskar et al. [10] investigated in-plane behavior of masonry infill walls with openings strengthened using textile reinforced mortar, Wang et al. [11], Wang et al. [12], Li et al. [13] investigated progressive collapse of self-centering precast concrete frame with infill walls, Ning et al. [14] studied earthquake performance of infilled reinforced concrete frames, Luo et al. [15] studied the impact of infill wall distribution on the mechanical behavior and failure patterns of multi-story RC frame structures, Li et al. [16] investigated seismic behavior of steel frame infilled with wall-panels connected by sliding joint, Zhang et al. [17] studied on improving cyclic behavior of infilled reinforced concrete frame by prefabricated wall panels with sliding joints, Balık et al. [18] investigated infill walled RC frames covered with steel sheets. On the other hand, there are also a few dynamic-based experimental studies on this subject. Nie et al. [19] studied progressive collapse of the double-layer cylindrical reticulated shell with infilled wall on shake table, Nicoletti et al. [20] studied the contribution of infill wall stiffness to steel frame structures, Yu et al. [21] investigated seismic behavior of hinged steel frames with masonry infill walls, Bahadır [22] studied band-type window spaces that can cause short-column and soft-story behaviors in RC structures on shake table experiments, Yousefianmoghadam et al. [23] investigated system identification of a two-story infilled RC building in 4 different damage states, damage was formed by removing infill walls. To summarize the literature review, there are studies on the effects of infill walls on RC structures. These are mostly static-based studies. There are a few dynamic-based studies. These studies have been conducted mainly on strengthening, strength, load carrying capacity and performance, and no research has been found on stiffness, especially on initial stiffness where the contribution of infill walls can be seen most clearly. This study addresses this gap in the literature.

In the study, the effect of infill walls on dynamic behavior in reinforced concrete structures was investigated. For this purpose, experimental modal analysis (EMA) was performed with shake table tests on the frame sample with and without infill walls. Since the main contribution of infill walls to the structure will be stiffness and it is known that the largest part of this contribution will be until the walls are damaged, no stiffness loss was desired in the sample and the experiments were performed in the elastic region. Thus, modal analysis calculations were not affected by instantaneous stiffness losses and modal parameters directly related to stiffness could be calculated clearly. Dynamic behaviors in two different states of the sample were determined by performing experimental modal analysis and load-displacement analyses and the effect of infill walls on the behavior was investigated. In addition, numerical modal analysis was performed with linear time history analysis under the same conditions for two different states of the sample using the ETABS finite element software.

2. MATERIAL AND METHODS

2.1. Sample Properties, Material Details and Construction

A 1/3 geometric scale 2-storey single-span 3D RC frame sample was constructed to be examined with vibration tests. The sample was named as (RS) in its empty-bare state (reference) and (IS) in its improved state with infill walls. The digital 3D views of the sample in RS and IS states are given in Figure 1. Some construction stages for the bare state of the sample are also shown in Figure 2. Some mistakes were made deliberately in the frame in order to represent the existing building stock. Some of these mistakes are insufficient concrete compressive strength [24], not making stirrup densification, not using stirrups in joint areas, not complying with the strong column-weak beam principle.

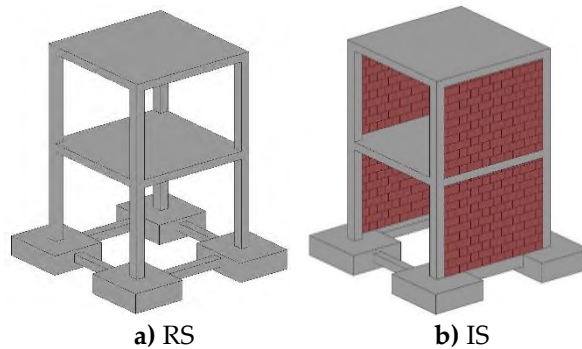


Figure 1. 3D views of the sample in two different states

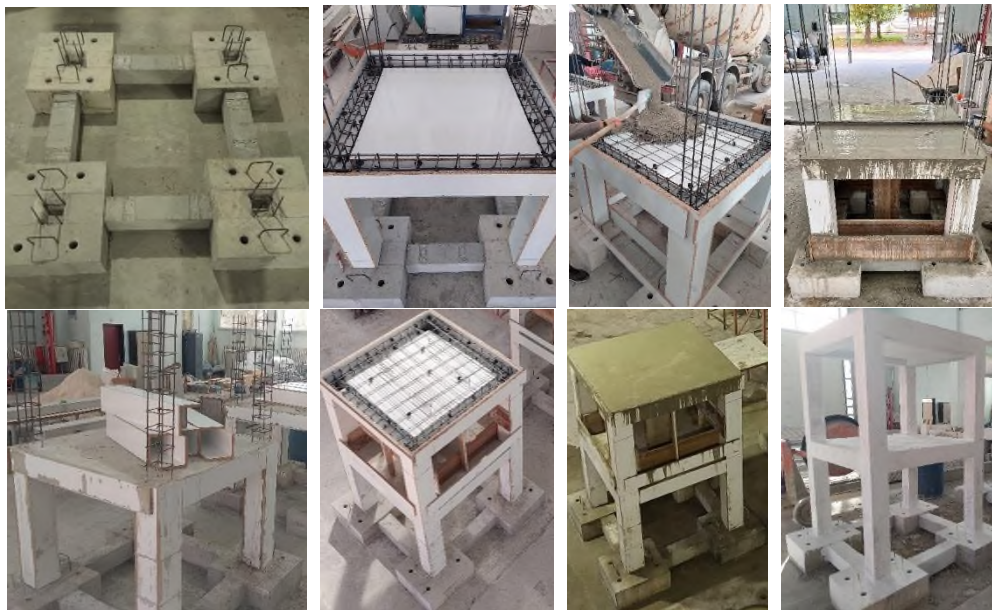


Figure 2. Construction stages

The cross-section dimensions of the columns and beams are 15×15 cm. The slabs in the sample are a type of two-way slab with beams and have a thickness of 8 cm. The foundation of the frame sample is strap footing. The story heights and the span lengths in both directions of the slabs are 1 m. The dimensions and views of the frame are as shown in Figure 3. The front and side views are exactly the same.

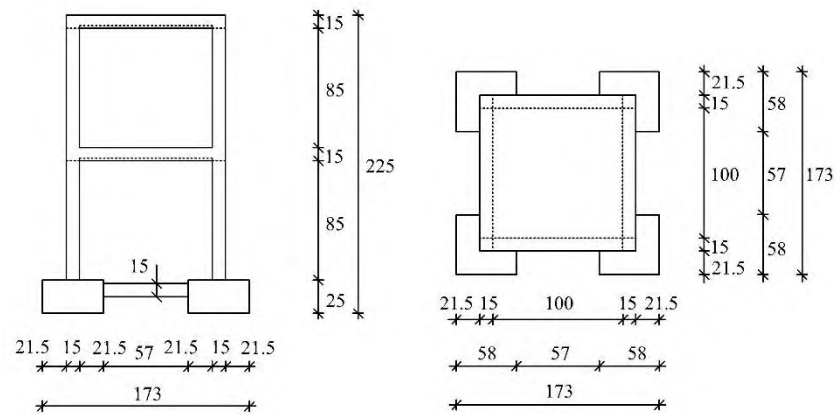


Figure 3. Dimensions and views of the sample; front and side view (left), top view (right) (All dimensions are in 'cm'.)

As a result of standard compression tests, the average concrete compressive strength in the stories of the sample was determined as 5.94 MPa and in the foundation as 21.11 MPa (Figure 4). Since the foundation will not be examined in the vibration tests, it is aimed to have high stiffness. [24]

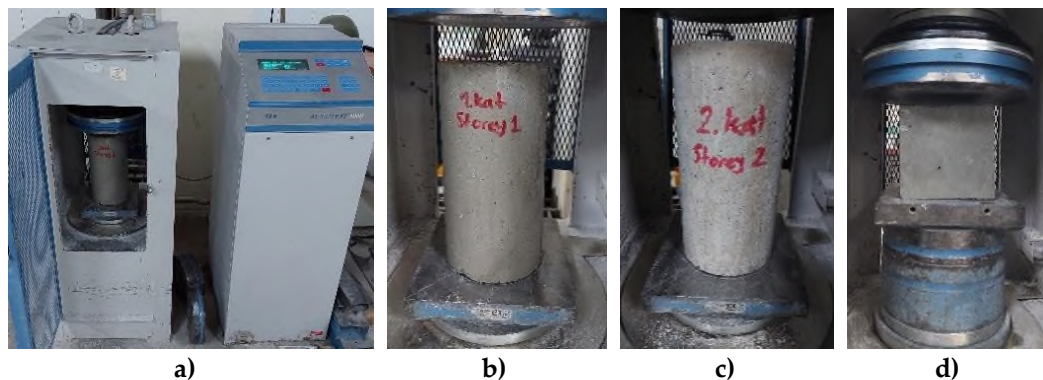


Figure 4. Standard compression tests; a) Test device, b) 1st story concrete sample, c) 2nd story concrete sample, d) Foundation concrete sample

The reinforcement details of the sample are given in Figure 5. The dimensions, reinforcement arrangements and details are the same in both horizontal directions. All reinforcement are ribbed steel with a yield strength of 420 MPa. The longitudinal reinforcement ratio in the columns was designed to deliberately not meet the minimum longitudinal reinforcement ratio requirement of 0.01 recommended by TBDY 2018 [1]. In the slabs, mesh reinforcement with a reinforcement diameter of 6 mm and 150×150 mm intervals was placed at the bottom and top of the section.

2.2. Experimental Setup

A shake table was used as an exciter in vibration experiments. The system can produce vibration in the horizontal direction by converting the rotational motion in the servo motor into linear motion. The platform dimensions of the system are 4×4 m. The shake table, which has a displacement capacity of ±153 mm in the horizontal direction, can carry a load of up to 10 tons in the vertical direction.

Responses were obtained by means of accelerometers and potentiometers. The sensors were placed in the same direction as the loading. Displacement measurements were made at a total of 3 different points, namely at the center of the foundation beam, and at the center of the beams on the 1st and 2nd stories. Similarly, acceleration measurements were made at a total of 3 points, namely 2 of them at the

center of the story beams and 1 on the platform. The digital drawing of the experimental setup is shown in Figure 6, and the actual view and sensor locations are shown in Figure 7.

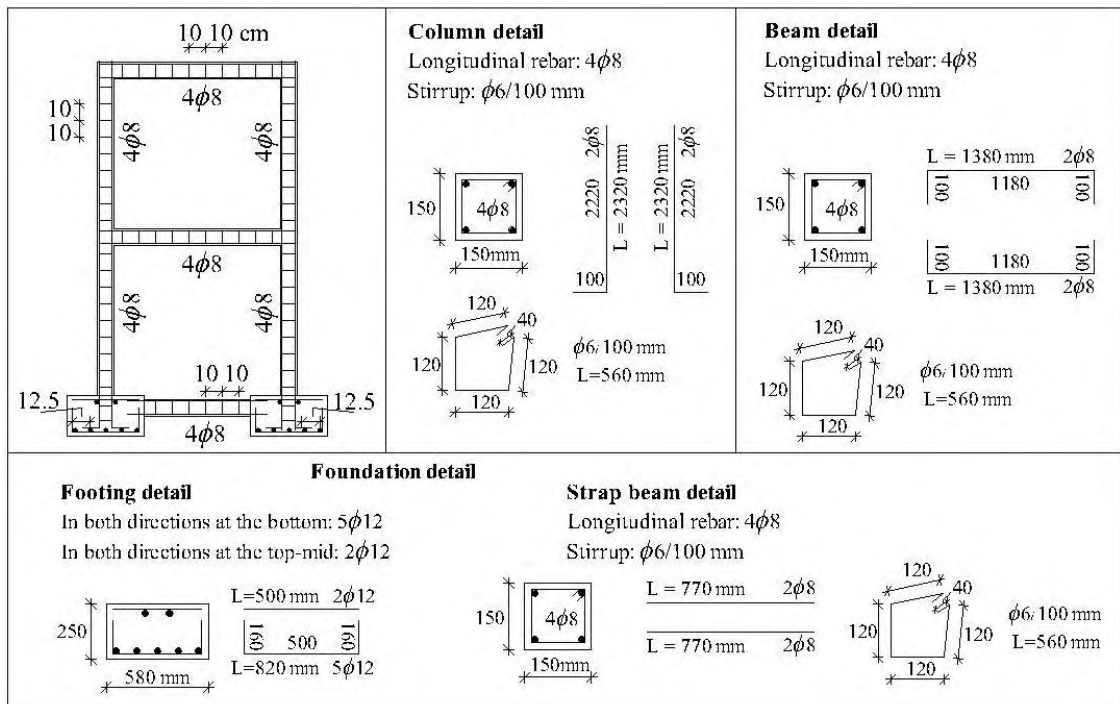


Figure 5. Reinforcement details

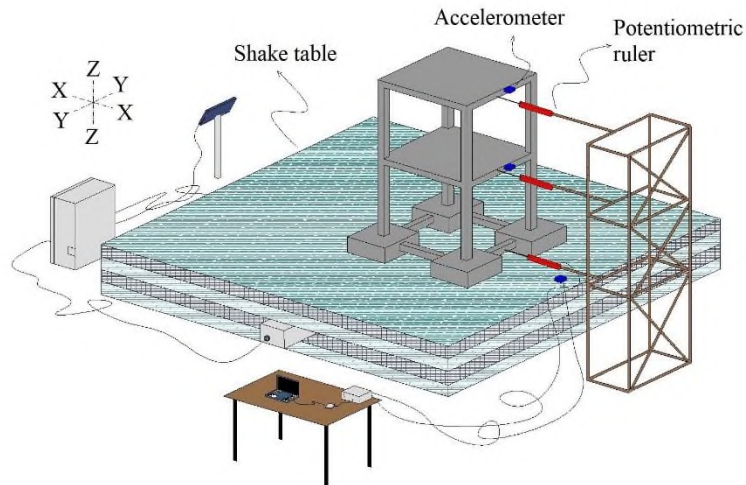


Figure 6. Digital drawing of the experimental setup



Figure 7. a) Experimental setup; 1) shake table, 2) control panel, 3) PLC-controlled automation system, 4) data acquisition system, 5) accelerometers, b) Sensor locations; 1) 1. story sensors, 2) 2. story sensors, 3) potentiometer on the foundation, 4) accelerometer on the shake table platform

2.3. Loading

In the experimental phase, approximately 1 ton weight was placed on the sample floors. Here, the vertical load carrying capacity of the shake table and the damage states that may occur in the samples are taken as basis. As dynamic loading, the 25-second part where the values are dominant in the acceleration data recorded in the 90° direction at the Kakogawa, Japan station of the 1995 Kobe, Japan earthquake was applied, but it was seen that the table could not fully reflect this data in the feedback acceleration measured on the shake table. For this reason, the excitation acceleration was not named as the Kobe earthquake, but was defined as an artificial ground motion. Accordingly, the peak ground acceleration (PGA) of this artificial motion is 0.54 g, its total duration is 21 s (Figure 8). The acceleration and displacement response spectra of this loading at 5% damping ratio are given in Figure 9.

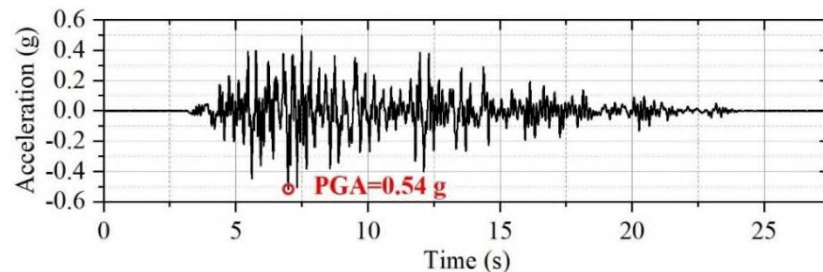


Figure 8. Dynamic excitation

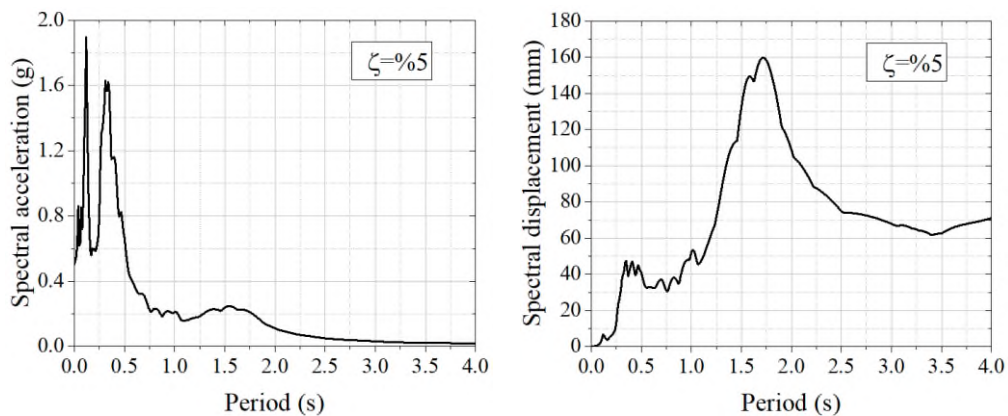


Figure 9. Acceleration response spectrum (left), displacement response spectrum (right)

2.4. Calculations Based on Experimental Data

Experimental modal analysis (EMA) was carried out using acceleration type frequency response functions (FRF, transfer function). First, signal processing was performed, and Blackman window was used to minimize the leakage error that would occur with Fast Fourier Transforms (FFT). Data were cut from appropriate frequency values with 4th order Butterworth type lowpass filter. Since no damage occurred in the sample during the experiments, at least 3 repeated tests could be performed for 2 different states of the sample. In this way, the average of FRF functions were created and, in this way, more reliable FRF graphs were obtained. Afterwards, erroneous data and noise were reduced, and nonlinear multi-degree of freedom Lorentzian type curve fitting was performed.

The natural frequencies of the 1st and 2nd modes in the loading direction were determined by the peak picking method from the resulting FRF amplitude graphs. The damping ratios were determined by the logarithmic decrement method from the top displacement-time graphs by taking into account the part where the forced vibration ends, and the free vibration begins. The mode shapes were also determined by the peak picking method from the imaginary FRF graphs.

Inertial forces occurring in the stories were taken as story shears and base shears were calculated accordingly [25], [26]. Lateral translational stiffness was determined via base shear-top displacement hysteresis curves. Here, stiffnesses were calculated by performing force/displacement on the curves obtained as a result of linear regression analysis. Since the frame was not damaged during the experiments and remained in the elastic region, these values were defined as initial lateral translational stiffnesses. [27]

In these stages, SeismoSignal v4.3.0 [28], OriginPro 2021 [29], Microsoft Excel [30], EasyTest Experimental Modal v2.1.5 [31] softwares were used.

2.5. Numerical Analysis

Numerical analysis was also performed for comparison with the experimental phase. Here, numerical analysis of the sample was performed under the same loading and the same conditions in the ETABS Ultimate v19.1.0 software according to the finite element method. Two different states of the sample were numerically examined with linear time history analysis. The finite element model of the sample for the RS and IS states is shown in Figure 10.

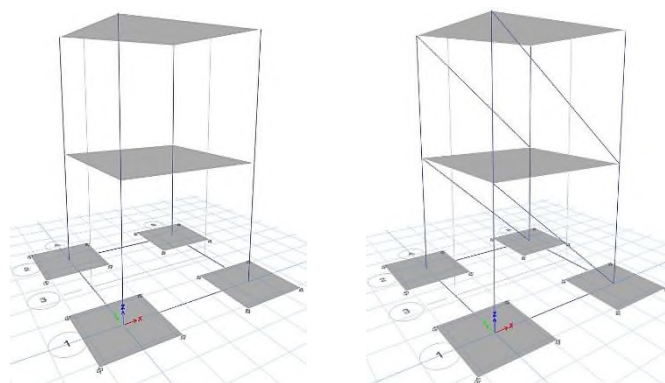


Figure 10. Finite element model of the sample; RS (left), IS (right) [32]

2.6. Experimental Phase

After the construction of the bare frame was completed, vibration experiments in the RS state were carried out. Experiment photos are shown in Figure 11.



Figure 11. RS state experiments

After the reference state experiments were completed, the improvement phase with infill walls was started. In this process, the frame openings of both floors in the loading direction of the sample were walled with bricks of 190×85×190 mm dimension. 1 week after the wall construction, the sample was plastered with a rough plaster of approximately 7.5 mm thickness from the inside and outside and as a result, the production of a 10 cm thick plastered infill wall was completed. The plastered areas were then cured with water for 7 days. The mortar material used in the wall and plaster consists of a mixture of cement, sand, water, and lime. Figure 12 shows the improvement process of the sample with infill walls.



Figure 12. Improvement with infill walls

After the infill wall production was completed, the tests of the sample in the improved with infill walls state (IS) were carried out in the same way. The test photos of the IS state are shown in Figure 13.



Figure 13. IS state experiments

3. RESULTS AND DISCUSSION

In this section, the experimentally obtained results are abbreviated as EXP, and the numerically obtained results with the ETABS program are abbreviated as NUM.

As expected, no visible damage/cracks were observed in either state of the sample during any of the tests. Accordingly, the sample remained in the elastic region in both RS and IS states and modal analysis could be carried out consistently for the initial state of the sample in both states.

Since the contribution of the infill walls to the lateral translational stiffness of the structure will decrease significantly in case of damage, the positive effect of the walls on the structure could be clearly observed without any loss of stiffness with elastic zone tests. Observations in the experiments showed that the lateral displacement of the sample decreased significantly in the IS state compared to the RS state due to the effect of the infill walls.

3.1. Modal Analysis

The curve-fitted accelerance type FRF amplitude graphs of the sample in the RS and IS states obtained as a result of the experimental modal analysis are given in Figure 14 and Figure 15. The natural frequencies of the sample in the 1st and 2nd lateral translational modes in the loading direction for the RS and IS states are given in Table 1 in the unit of 'Hz' and the natural periods in the unit of 's' are given in Table 2.

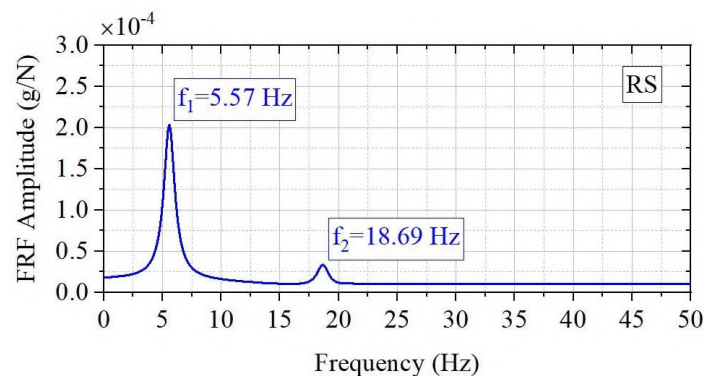


Figure 14. FRF amplitude graph of the sample in RS state

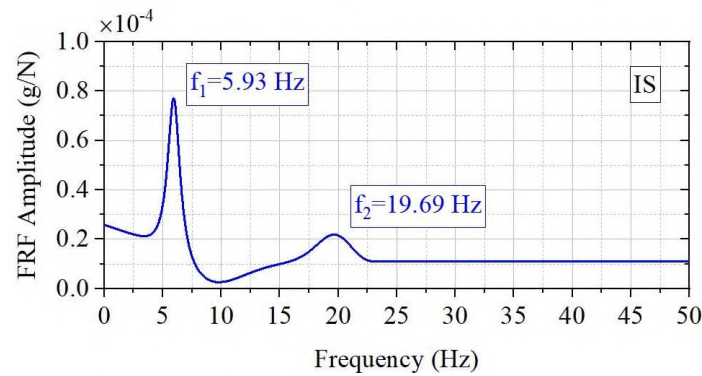


Figure 15. FRF amplitude graph of the sample in IS state

Table 1. Natural frequencies (Hz)

State	1. Mode (EXP)	1. Mode (NUM)	Difference	2. Mode (EXP)	2. Mode (NUM)	Difference
RS	5.57	5.45	2%	18.69	18.43	1%
IS	5.93	5.76	3%	19.69	18.54	6%

Table 2. Natural periods (s)

State	1. Mode (EXP)	1. Mode (NUM)	Difference	2. Mode (EXP)	2. Mode (NUM)	Difference
RS	0.180	0.184	2%	0.054	0.054	0%
IS	0.169	0.174	3%	0.051	0.052	2%

When Table 1 and Table 2 are examined, the experimentally obtained results and the numerically obtained results are quite close to each other.

The experimentally determined natural frequency and natural period values are compared in Table 3 for two different states of the sample.

Table 3. Comparison of natural frequencies and natural periods

Mode	Natural frequency (Hz) (EXP)			Natural period (s) (EXP)		
	RS	IS	Difference	RS	IS	Difference
1. Mode	5.57	5.93	+7%	0.180	0.169	-6%
2. Mode	18.69	19.69	+5%	0.054	0.051	-6%

According to Table 3, in the IS state, due to the effect of infill walls, the 1st natural frequency increased by 7% and the 2nd natural frequency increased by 5% compared to the RS state. The natural period values decreased by 6% for both modes. If Equation 1 is examined, the increase in frequency values can be achieved by increasing the stiffness or decreasing the mass. Here, it is understood that the stiffness increases because the mass is constant. In short, according to this result, the infill walls increased the stiffness of the frame.

Global damping ratios were determined by the logarithmic decrement method by considering the part where free vibration starts in the top displacement-time graphs based on experimental data. Accordingly, the damping ratios of the sample in the loading direction were calculated as 4.92% for the RS state and 4.10% for the IS state. Considering Equation 1 used in the damping ratio calculation, the decrease in the damping ratio with the increase in stiffness was a reasonable result [33]. Here, the global damping ratio decreased by 17% due to the increase in the lateral translational stiffness of the frame by the infill walls.

$$\omega_n^2 = k/m \quad \zeta = \frac{c}{2m\omega_n} \quad (1)$$

In the equation, ω_n represents the natural frequency, k represents the stiffness, m represents the mass, ζ represents the damping ratio, c represents the damping constant and c_{cr} represents the critical damping constant.

The 1st and 2nd lateral translational mode shapes obtained for the loading direction as a result of the numerical modal analysis are given in Figure 16.

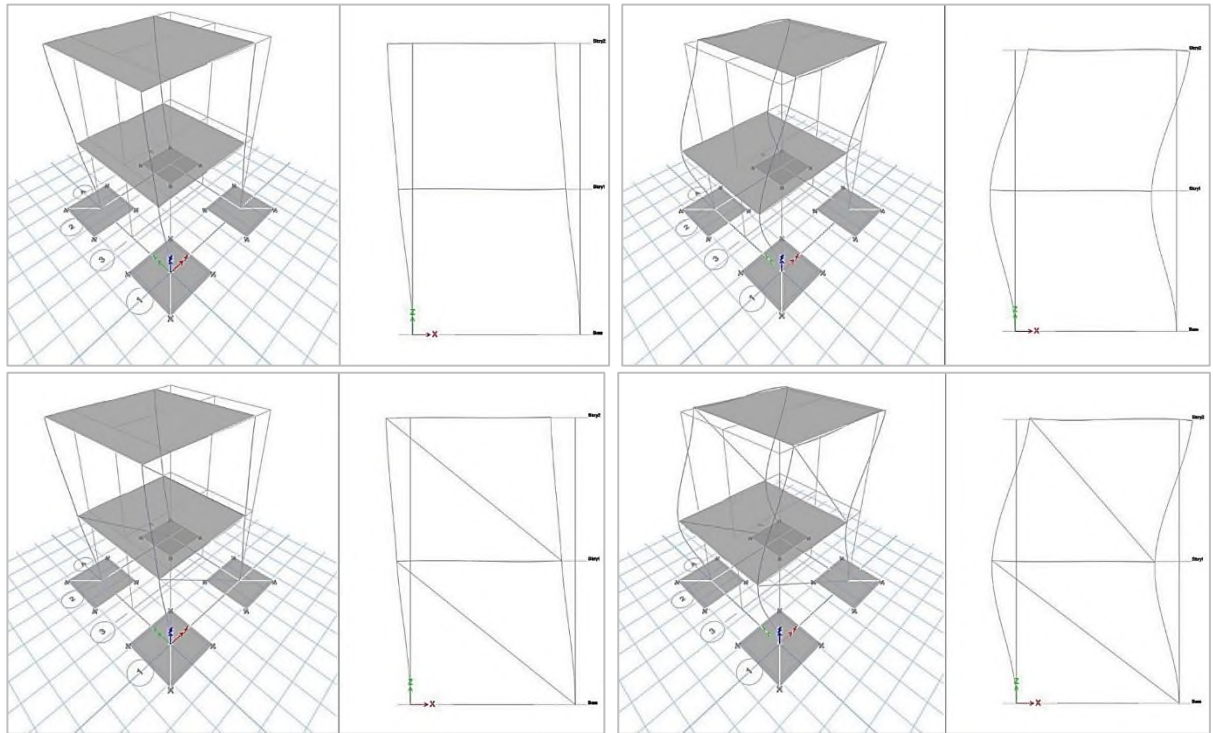


Figure 16. Mode shapes obtained as a result of numerical modal analysis; RS 1st Mode (top left), RS 2nd Mode (top right), IS 1st Mode (bottom left), IS 2nd Mode (bottom right) [32]

The 1st and 2nd lateral translational mode shapes determined by experimental and numerical modal analysis for the RS and IS states of the sample are compared in Figure 17 and Figure 18.

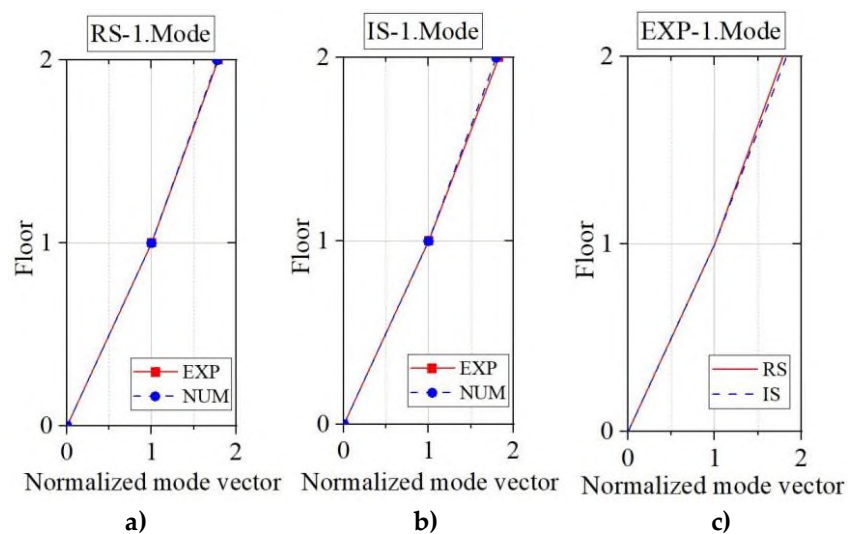


Figure 17. Comparison of lateral translational mode shapes; a) RS 1. Mode, b) IS 1. Mode, c) EXP 1.Mode

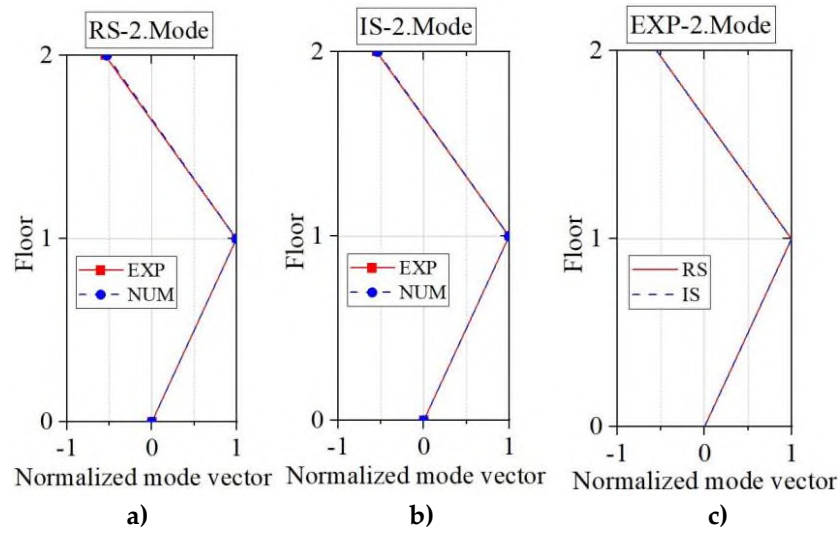


Figure 18. Comparison of lateral translational mode shapes; **a)** RS 2. Mode, **b)** IS 2. Mode, **c)** EXP 2. Mode

When Figure 17 and Figure 18 are examined, it is seen that the experimental and numerical results are quite compatible in terms of mode shapes. It is also seen that the infill walls do not have a significant effect on the lateral translational mode shapes.

3.2. Load-Displacement

The top displacement in time domain graphs obtained experimentally and numerically for the RS reference state and the IS infill walled state of the sample are given in Figure 19.

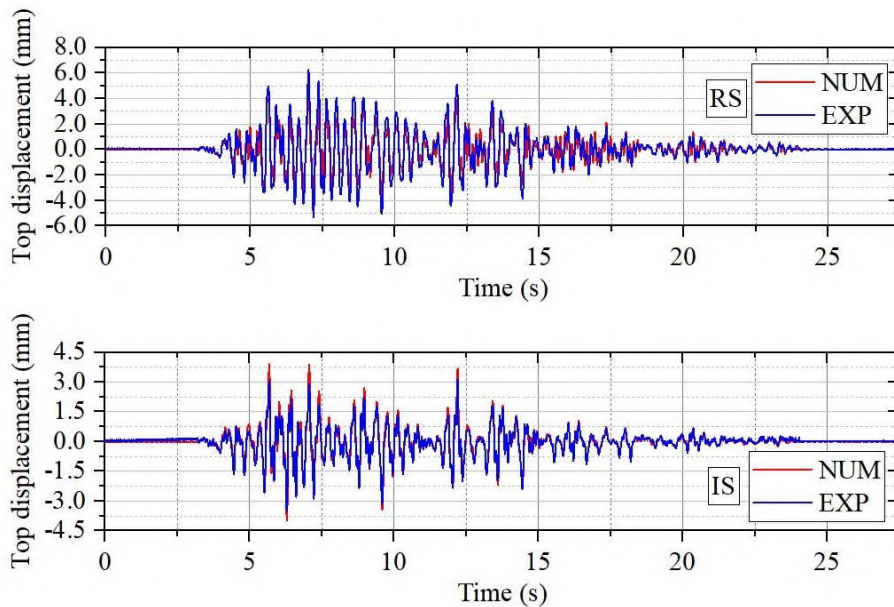


Figure 19. Top displacement-time graphs; RS (top), IS (bottom)

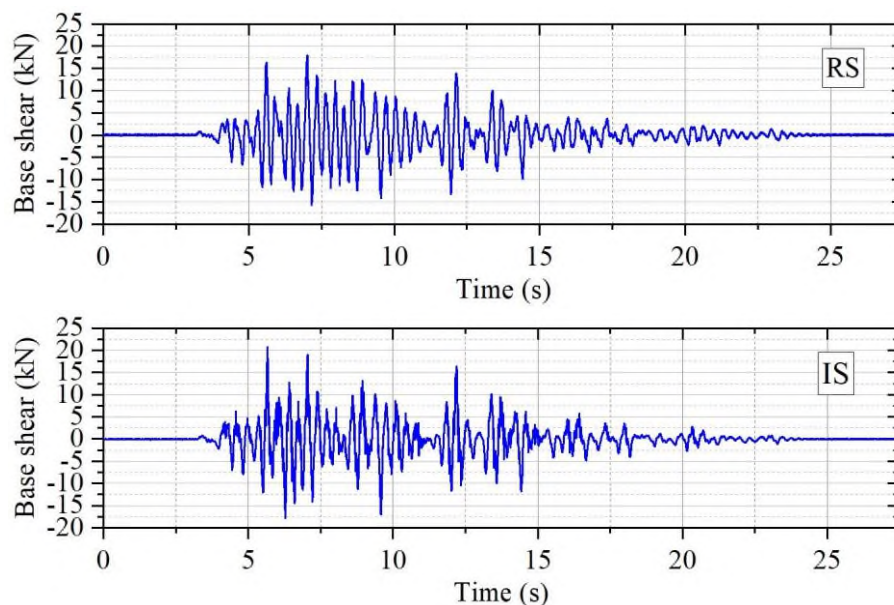
The absolute maximum top displacements of the frame determined experimentally and numerically in the RS and IS states are shown and compared in Table 4.

Table 4. Absolute maximum top displacements (mm)

	RS	IS	Difference
EXP	6.13	3.52	-43%
NUM	5.91	3.97	-33%
Difference	4%	13%	-

When Table 4 is examined, it is seen that the infill walls limit the absolute maximum top displacement to a great extent. Accordingly, the absolute maximum top displacement decreased by 43% in the IS state according to the experimental results and by 33% according to the numerical results compared to the RS state. In addition, there was a difference of 4% in the RS state and 13% in the IS state between the experimental and numerical results. These results show that infill walls significantly increase the frame stiffness and thus limit the displacements.

Experimentally obtained base shear-time graphs for the RS and IS states of the sample are given in Figure 20.

**Figure 20.** Base shear-time graphs; RS (top), IS (bottom)

The absolute maximum base shear values obtained experimentally were around 20 kN for both states of the sample.

The base shear-top displacement hysteresis curves created for the RS and IS states of the sample are shown and compared in Figure 21. In addition, curve fitting was performed on the hysteresis curves using linear regression analysis.

When Figure 21 is examined, it is seen that there is no tendency for the base shears to decrease, that is, the sample continues to receive loads without losing strength in both states and therefore remains in the elastic region. In addition, there are great differences in the slopes of the hysteresis curves. This situation is even clearer in the curves obtained as a result of linear regression analysis. The slope of the hysteresis curve is greater in the IS state than in the RS state. Since the slope here shows the force/displacement ratio, it directly corresponds to the lateral translational stiffness. In other words, the initial lateral translational stiffness of the sample has increased due to the effect of the infill walls. If we express it numerically, the stiffness value, which was 2.57 kN/mm in the RS state, became 4.82 kN/mm in the IS state. Thus, an 88% increase in stiffness has occurred thanks to the positive effect of the infill walls on the structure.

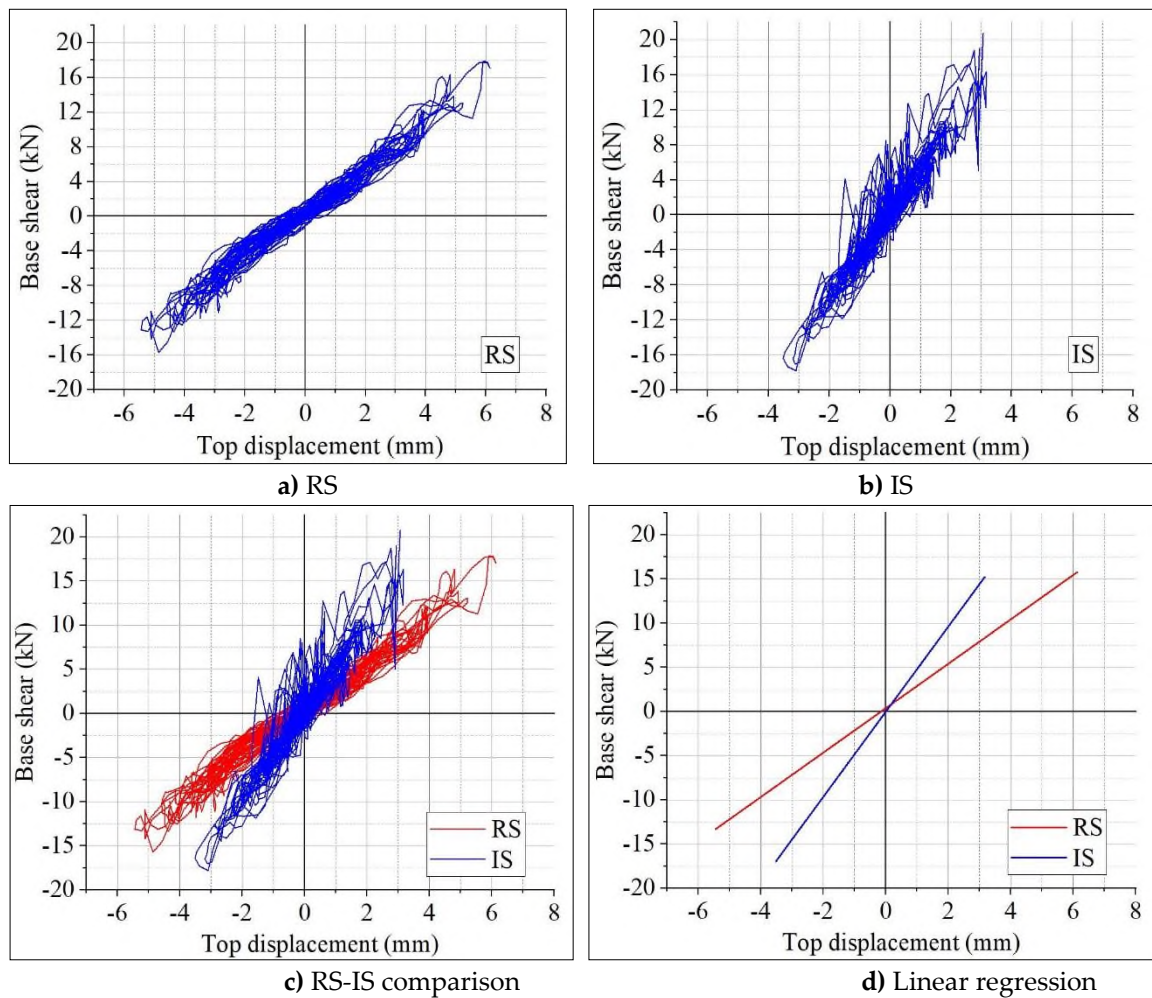


Figure 21. Base shear-top displacement hysteresis curves; **a)** RS, **b)** IS, **c)** RS-IS comparison, **d)** Linear regression

4. CONCLUSIONS

In this study, the effect of infill walls on dynamic behavior in RC structures was investigated experimentally and numerically. Shake table tests were performed on a 3D RC frame with 1/3 scale 2 stories and single-span with and without infill walls. Dynamic parameters were determined for these two different states through experimental modal analysis and load-displacement analyses were performed using experimental data. In addition, numerical analysis was performed under the same conditions with the ETABS finite element software.

The results and comparisons obtained as a result of experimental and numerical studies are given below.

1. Infill walls increased the lateral translational stiffness of the frame and in this way, the modal parameters and displacements which are directly related to stiffness were significantly changed. Here, thanks to the stiffness gain, frequency values increased, periods, damping ratios, top displacements decreased, and thus significant contributions were made to the dynamic behavior of the frame.
2. Mode shapes and base shear are not affected much by the addition of infill walls. The fact that the base shear is similar in the cases with and without infill walls indicates that the contribution of the walls to the strength in the elastic region is very limited. If the behavior in the plastic

region is also considered, the expected increase to the strength according to TBEC 2018 [1] is already at most 15%.

3. In the experiments, it was observed that the lateral displacement of the sample decreased significantly in the IS state compared to the RS state due to the effect of infill walls.
4. In the IS state, the 1st natural frequency of the sample increased by 7% (5.57 Hz to 5.93 Hz) and the 2nd natural frequency increased by 5% (18.69 Hz to 19.69 Hz) compared to the RS state.
5. 1st natural periods are 0.180 s and 0.169 s, 2nd natural periods are 0.054 s and 0.051 s for RS and IS states, respectively. There is a 6% difference in the 1st and 2nd natural period values between the states of the sample.
6. According to logarithmic decrement method, in the IS state, the global damping ratio was determined to be 17% less than in the RS state (4.92% to 4.10%). According to this result, it is seen that there is an inverse proportion between stiffness and damping ratio.
7. According to the experimental results, infill walls reduced the top displacement by 43% (6.13 mm to 3.52 mm) and according to the numerical results, by 33% (5.91 mm to 3.97 mm). These values indicate a significant gain in stiffness.
8. There was a great difference in the slopes of the base shear-top displacement hysteresis curves (force/displacement), i.e. lateral translational stiffnesses, between the RS and IS states. Infill walls increased the initial lateral translational stiffness of the sample by 88%.
9. Numerical analysis yielded results that were remarkably close to the experimental results.

Considering these results, it has been determined that infill walls provide a significant increase in the initial lateral translational stiffness, thus limiting the displacement demand to a great extent, increasing the natural frequencies substantially and reducing the damping ratio significantly. Thus, it is obvious that infill walls have a significant effect on the dynamic behavior of RC structures under earthquake effects and their contributions, especially in the elastic region, should not be ignored.

Declaration of Ethical Standards

The authors declare that they followed all ethical guidelines including authorship, citation, data reporting, and publishing original research.

Credit Authorship Contribution Statement

Author 1: conceptualization, methodology, formal analysis and investigation, writing-original draft preparation, writing-review and editing.

Author 2: conceptualization, writing-review and editing, funding acquisition, resources, supervision.

Declaration of Competing Interest

The authors declare that they have no financial conflicts of interest or personal relationships that could have influenced the work presented in this manuscript.

Funding / Acknowledgements

This study is part of the doctoral dissertation of the first author, which was accepted by the KTUN Graduate Education Institute in 2024. The dissertation was funded by the KTUN Coordinatorship of the Instructor Training Programme (2018-ÖYP-42). The authors wish to express their gratitude to the KTUN Coordinatorship of the Instructor Training Programme for their collaboration.

5. REFERENCES

- [1] Republic of Türkiye Ministry of Interior Disaster and Emergency Management Presidency, *TBEC 2018 – Turkish Building Earthquake Code 2018*. Ankara, Türkiye, 2018.
- [2] A. S. Aljawadi, M. Vafaei, S. C. Alih, “Seismic strengthening of deficient ground soft-story RC frames with inadequate lap splice using chevron brace,” *Structures*, vol. 61, pp. 106029, 2024. <https://doi.org/10.1016/j.istruc.2024.106029>.
- [3] S. Yang, S. Zheng, L. Dong, L. Liu, Y. Xiao, W. Zhao, “Seismic performance of corroded reinforced concrete short columns: Experiment and theoretical analysis,” *Structures*, vol. 70, pp. 107665, 2024. <https://doi.org/10.1016/j.istruc.2024.107665>.
- [4] Z. Celep, *Structural dynamics*, 4th ed., İstanbul: Beta Printing and Publishing, 2011. (in Turkish)
- [5] X. Zhang, Y. Zhou, X. Liu, C. Wang, Z. Sun, “Study on failure mechanism and seismic performance of RC Frame-Infilled walls structures reinforced by CFRP,” *Eng Fail Anal*, vol. 168, pp. 109114, 2025. <https://doi.org/10.1016/j.engfailanal.2024.109114>.
- [6] Y. C. Ou, N. V. B. Nguyen, L. Hoang, “Cyclic behavior and pushover analysis of large scale two-bay, two-story reinforced concrete frames infilled with walls with openings,” *Eng Struct*, vol. 317, pp. 118663, 2024. <https://doi.org/10.1016/j.engstruct.2024.118663>.
- [7] W. Jin, C. Zhai, M. Zhang, W. Liu, Y. Wei, L. Xie, “Experimental investigation on the in-plane and out-of-plane interaction of isolated infills in RC frames,” *Eng Struct*, vol. 293, pp. 116569, 2023. <https://doi.org/10.1016/j.engstruct.2023.116569>.
- [8] S. Pradhan, Y. Sanada, Y. Rokhyun, H. Choi, K. Jin, “Effects of passive confinement on out-of-plane robustness of unreinforced masonry infill walls,” *Structures*, vol. 65, pp. 106676, 2024. <https://doi.org/10.1016/j.istruc.2024.106676>.
- [9] J. Monical, S. Pujol, “A study of the response of reinforced concrete frames with and without masonry infill walls to earthquake motions,” *Structures*, vol. 63, pp. 106345, 2024. <https://doi.org/10.1016/j.istruc.2024.106345>.
- [10] J. K. Bhaskar, D. Bhunia, L. Koutas, “In-plane behaviour of masonry infill walls with openings strengthened using textile reinforced mortar,” *Structures*, vol. 63, pp. 106439, 2024. <https://doi.org/10.1016/j.istruc.2024.106439>.
- [11] H. Wang, S. Li, C. Zhai, “Experimental and numerical investigation on progressive collapse of self-centering precast concrete frame with infill walls,” *J Build Eng*, vol. 78, pp. 107472, 2023. <https://doi.org/10.1016/j.jobe.2023.107472>.
- [12] H. Wang, S. Li, C. Zhai, “Effect of infill walls on progressive collapse behavior of self-centering precast concrete frame,” *Structures*, vol. 59, pp. 105729, 2024. <https://doi.org/10.1016/j.istruc.2023.105729>.
- [13] S. Li, H. Wang, H. Liu, S. Shan, C. Zhai, “Experimental study on progressive collapse of self-centering precast concrete frame with infill walls,” *Eng Struct*, vol. 294, pp. 116746, 2023. <https://doi.org/10.1016/j.engstruct.2023.116746>.
- [14] N. Ning, Z. J. Ma, P. Zhang, D. Yu, J. Wang, “Influence of masonry infills on seismic response of RC frames under low frequency cyclic load,” *Eng Struct*, vol. 183, pp. 70-82, 2019. <https://doi.org/10.1016/j.engstruct.2018.12.083>.
- [15] R. Luo, X. Guo, B. Wang, X. Dong, Q. Zhang, Z. Quyang, “The impact of infill wall distribution on the mechanical behavior and failure patterns of multi-story RC frame structures: An acceleration strain coupled testing approach,” *Structures*, vol. 59, pp. 105737, 2024. <https://doi.org/10.1016/j.istruc.2023.105737>.
- [16] Y. Li, Z. Ning, H. L. Shan, C. M. Gao, S. Huang, “Seismic behavior of steel frame infilled with wall-panels connected by sliding joint,” *J Constr Steel Res*, vol. 212, pp. 108253, 2024. <https://doi.org/10.1016/j.jcsr.2023.108253>.
- [17] C. Zhang, Z. Yang, T. Yu, W. Huang, X. Deng, Z. Lin, S. Wu, “Experimental and numerical studies of improving cyclic behavior of infilled reinforced concrete frame by prefabricated wall

- panels with sliding joints," *J Build Eng*, vol. 77, pp. 107524, 2023. <https://doi.org/10.1016/j.jobbe.2023.107524>.
- [18] F. S. Balık, F. Bahadır, M. Kamanlı, "Seismic behavior of lap splice reinforced concrete frames with light-steel-framed walls and different anchorage details," *Struct Eng Int*, vol. 33, no. 3, pp. 488-497, 2023. <https://doi.org/10.1080/10168664.2022.2073941>.
- [19] G. B. Nie, Y. J. Shi, C. X. Zheng, Z. Y. Wang, W. Wang, Q. S. Yang, "Shaking table test on progressive collapse of the double-layer cylindrical reticulated shell with infilled wall," *Structures*, vol. 67, pp. 106946, 2024. <https://doi.org/10.1016/j.istruc.2024.106946>.
- [20] V. Nicoletti, L. Tentella, S. Carbonari, F. Gara, "Stiffness contribution and damage index of infills in steel frames considering moderate earthquake-induced damage," *Structures*, vol. 69, pp. 107581, 2024. <https://doi.org/10.1016/j.istruc.2024.107581>.
- [21] Q. Q. Yu, J. Y. Wu, X. L. Gu, L. Wang, "Seismic behavior of hinged steel frames with masonry infill walls," *J Build Eng*, vol. 77, pp. 107536, 2023. <https://doi.org/10.1016/j.jobbe.2023.107536>.
- [22] F. Bahadır, "Experimental study on three-dimensional reinforced concrete frames subjected to dynamic loading," *Structures*, vol. 24, pp. 835-850, 2020. <https://doi.org/10.1016/j.istruc.2020.01.045>.
- [23] S. Yousefianmoghadam, M. Song, A. Stavridis, B. Moaveni, "System identification of a two-story infilled RC building in different damage states," *Improving the Seismic Performance of Existing Buildings and Other Structures*, pp. 607-618, 2015. <https://doi.org/10.1061/9780784479728.050>.
- [24] M. Inel, S. M. Senel, H. Un, "Experimental evaluation of concrete strength in existing buildings," *Magazine of Concrete Research*, vol. 60, pp. 279-289, 2008. <https://doi.org/10.1680/macr.2007.00091>.
- [25] I. Khan, K. Shahzada, T. Bibi, A. Ahmed, H. Ullah, "Seismic performance evaluation of crumb rubber concrete frame structure using shake table test," *Structures*, vol. 30, pp. 41-49, 2021. <https://doi.org/10.1016/j.istruc.2021.01.003>.
- [26] S. Gavridou, J. W. Wallace, T. Nagae, T. Matsumori, K. Tahara, K. Fukuyama, "Shake-table test of a full-scale 4-story precast concrete building. I: Overview and experimental results," *J Struct Eng*, vol. 143, no. 6, pp. 04017034, 2017. [https://doi.org/10.1061/\(ASCE\)ST.1943-541X.0001755](https://doi.org/10.1061/(ASCE)ST.1943-541X.0001755).
- [27] A. G. El-Attar, R. N. White, P. Gergely, "Shake table test of a 1/8 scale three-story lightly reinforced concrete building," National Center for Earthquake Engineering Research, Cornell University, USA, Tech. Report. 1991:NCEER-91-0018.
- [28] *SeismoSignal v4.3.0*. Seismosoft Ltd., 2011.
- [29] *OriginPro*, Northampton, Massachusetts: OriginLab Corporation, 2021.
- [30] Microsoft Office 365, *Microsoft Excel*, Redmond, Washington: Microsoft Corporation.
- [31] *EasyTest Experimental Modal v2.1.5*, Ankara: Teknik Destek Grubu Ltd., 2023.
- [32] *ETABS Ultimate v19.1.0*, Berkeley, California: Computers and Structures Inc., 2021.
- [33] A. K. Chopra, *Dynamics of structures: Theory and applications to earthquake engineering*, 4th ed., London: Pearson Education Ltd., 2012.